HOKKAIDO UNIVERSITY

Title	Thermogravimetric analysis and microstructural observations on the formation of GaN from the reaction between Ga2O3 and NH3
Author(s)	Kiyono, Hajime; Sakai, Toshiki; Takahashi, Mari et al.
Citation	Journal of Crystal Growth, 312(19), 2823-2827 https://doi.org/10.1016/j.jcrysgro.2010.06.021
Issue Date	2010-09-15
Doc URL	https://hdl.handle.net/2115/44033
Type	journal article
File Information	JCG312-19_2823-2827.pdf

Hokkaido University Collection of Scholarly and Academic Papers : HUSCAP

Thermogravimetric analysis and microstructural observations on the formation of GaN from the reaction between Ga_2O_3 and NH_3

Hajime Kiyono*, Toshiki Sakai, Mari Takahashi, and Shiro Shimada
Graduate School of Engineering, Hokkaido University, Sapporo, 060-8628, JAPAN

Abstract

Thermogravimetric analysis (TGA) and microstructural observations were carried to investigate the nitridation mechanism of β-Ga_2O_3 powder to GaN under an NH_3/Ar atmosphere. Non-isothermal TGA showed that nitridation of β-Ga_2O_3 starts at ~650 °C, followed by decomposition of GaN at ~1100 °C. Isothermal TGA showed that nitridation follows linear kinetics in the temperature range 800–1000 °C. At an early stage of nitridation, small GaN particles (~5 nm) are deposited on the β-Ga_2O_3 crystal surface, and they increase with time. We proposed a mechanism for the nitridation of Ga_2O_3 by NH_3 whereby nitridation of β-Ga_2O_3 proceeds via the intermediate vapor species Ga_2O (g).

Keywords: A1, Growth models, A2. Growth from vapor, B1. Nitrides

PACS: 81.10.St Growth in controlled gaseous atmospheres

1. **Introduction**

Gallium nitride (GaN) is a promising wide-band gap semiconductor used in manufacturing light emitting diodes, laser diodes, and ultra-violet photo detectors. [1–3] GaN epilayers are usually fabricated by chemical vapor deposition using metal-organic gallium compounds. In general, such metal-organic compounds are expensive and difficult to handle in air, another method to fabricate GaN has been needed. It has been reported that GaN powders can be also prepared by nitridation of Ga_2O_3 by NH_3. [4–7] Recently, GaN epilayers, nanotubes, and nanobelts have been produced by this method. [8–11] In addition, bulk GaN crystals have been synthesized by carbothermal reduction and nitridation of β-Ga_2O_3 by NH_3. [12–15] These results indicate that the nitridation of Ga_2O_3 by NH_3 is an important method for fabricating GaN materials. The overall reaction for nitridation of Ga_2O_3 by NH_3 is as follows:

$$Ga_2O_3 + 2NH_3 \rightarrow 2GaN + 3H_2O \quad (1)$$

Balkas et al. pointed out, on the basis of thermodynamic calculations, that reaction (1) does not occur directly but rather through intermediate gaseous species of Ga_2O (g). They suggested that GaN is formed by the reaction between NH_3 and the gaseous Ga_2O. [6] Luo et al. also suggested the formation of gaseous Ga_2O as an intermediate species by reaction

between β-Ga_2O_3 and H-containing species that are formed by thermal decomposition of NH_3. Jung et al. suggested the nitridation of β-Ga_2O_3 by NH_3 proceeds via solid state species such as GaO_xN_y (s). [16, 17] From the previous studies, it can be concluded that the mechanism of Ga_2O_3 nitridation by NH_3 is still not clear. Usually, the kinetics of a chemical reaction provides information about its mechanism. The present study investigates the nitridation of β-Ga_2O_3 to GaN by NH_3 on the basis of kinetic results using thermogravimetric analysis (TGA) and microstructural observations; a nitridation mechanism is proposed.

2. Experimental procedures

2.1 β-Ga_2O_3 powder

Commercially available β-Ga_2O_3 powder (99.9% purity; Koujyundo Kagaku Co.) was used for the nitridation. Figure 1(a) shows the scanning electron microscopic (SEM) images of as-received β-Ga_2O_3 powder. The powder contains secondary particles about 1–10 μm long consisting of primary particles of about 0.1 μm in size. When as-received β-Ga_2O_3 powder was sintered at 1400 °C for 1 h in Ar, β-Ga_2O_3 powders were coarsened as a result of the growth of primary particles, accompanied by diminishing pore size (Fig. 1 (b)). The secondary particle sizes were almost same as those of the as-received powder. The sintered powder was also used for the nitridation. The specific surface area of the as-received and

coarse β-Ga_2O_3 powder was about 10 and 1 m^2/g, respectively, as measured by the BET method using N_2 gas (BELSORP-mini, BEL JAPAN,).

2.2 Thermogravimetric analysis and microstructural observations

The weight change during nitridation was continuously monitored by an electric micro balance (Cahn D200). The β-Ga_2O_3 powder was placed in an alumina cell, which was hung with alumina wires with about 40 cm long in total and located in a fused quartz tube in a vertical furnace. Mixed gases of NH_3/Ar (10/90, 50/50, 90/10 kPa), H_2/Ar (40/60 kPa), or Ar (100 kPa) at a total flow rate of 100 mL/min were introduced at the top of the tube. Non-isothermal nitridation was carried out by heating β-Ga_2O_3 to 1200 °C at a rate of 5 °C /min, while isothermal nitridation was carried out at a temperature 800–1000 °C for about 1 h. In the non-isothermal nitridation, the exhaust gas from the TG system was analyzed by a mass-spectrometer (VG GAS ANALYZER, FISONS). The sampling point of the exhaust gas was about 20 cm downstream from the sample holder, where the gas was cooled to room temperature. The nitrided samples from both non-isothermal and isothermal TGA were characterized by X-ray powder diffraction (XRD, RINT 2000, RIGAKU), SEM (JSM-6300F, JEOL), and high-resolution TEM-SEM (HD-2000, HITACHI). The residual oxygen in the sample was determined using an oxygen and nitrogen analyzer (EMGA-620W, HORIBA).

3. Results and Discussion

3.1 The results of thermogravimetrical analysis

Non-isothermal TGA results of as-received β-Ga_2O_3 powder obtained by heating to 1200 °C in NH_3/Ar (50/50 kPa), H_2/Ar (40/60 kPa), and Ar atmospheres are shown in Fig. 2. No weight change was observed in the Ar atmosphere over the entire temperature range (20–1200 °C); suggesting that vaporization of β-Ga_2O_3 powder does not occur in that temperature range. In H_2/Ar (40/60 kPa), the weight loss starts at ~800 °C. On the basis of thermodynamic calculations, Butto et al. suggested that Ga_2O (g) is formed as a main product above 720 °C by the reaction between Ga_2O_3(s) and H_2 given as follows:[18]

$$Ga_2O_3\,(s) + 2H_2\,(g) \rightarrow Ga_2O\,(g) + 2H_2O\,(g) \quad (2)$$

Apparently, the weight loss in an H_2/Ar atmosphere is caused by the generation of Ga_2O (g) by partial decomposition or reduction of β-Ga_2O_3. In NH_3/Ar (50/50 kPa), the weight loss starts at ~650 °C and decreases to −10 wt%, reaching a short plateau at ~870°C (first weight loss). After the plateau, the weight decreases further, starting around 1000 °C, and becomes significant above 1100 °C (second weight loss). Figure 3 shows the XRD patterns for as-received β-Ga_2O_3 powder and for the sample heated to 870 °C and 1200 °C in Ar/NH_3 (50/50 kPa). This indicates that β-Ga_2O_3 begins to change to a wurtzite-type GaN above 870 °C,

the latter becoming well-crystallized at 1200 °C. The weight loss due to the complete nitridation of β-Ga_2O_3 to GaN in Eq (1) is calculated to be −10.6%. A relatively good agreement between the first weight loss and the calculated one for the complete nitridation showed that the first weight loss is caused by the complete nitridation of β-Ga_2O_3 to GaN. The second weight loss after the plateau (>1000 °C) resulted from decomposition of GaN in NH_3. In the non-isothermal experiment in NH_3/Ar and H_2/Ar atmospheres, gas species containing Ga (> 69.7 in mass number) in the exhaust gas were not detected by the mass-spectroscopic analysis.

The kinetic results by isothermal TGA for the nitridation of as-received β-Ga_2O_3 powder in the temperature range 800–1000 °C are shown in Fig. 4. After the TG analysis, no deposit was observed at the outside wall of sample cell, hanging wires or inner wall of a furnace tube. Over this temperature range, the weight loss from −1% to −9% occurs linearly with time (dashed lines). The samples obtained at the weight loss of −10% over the entire temperature range gave only GaN peaks on XRD, indicating the nitridation of β-Ga_2O_3 by NH_3 according to Eq (1). The close-to-linear weight loss curve suggests that the nitridation is limited by an interfacial reaction.

$$\Delta W / W_{\text{theo}} \times 100 = kt \qquad (3)$$

where, ΔW is the observed weight loss, W_{theo} the theoretical weight loss when the nitridation is completed (−10.6%), k the rate constant, and t the reaction time. From the slope of the linear region, k was calculated at each temperature. The Arrhenius plots of the k value provide activation energy of 110 kJ mol^{-1} for nitridation reaction. The weight loss reduced after -9%, barely approaching the theoretical weight loss (−10.6%) due to the characteristic of complete nitridation. The sample obtained after the isothermal nitridation at 1000 °C actually contained about 4 wt% oxygen, suggesting the difficulty in complete removal of oxygen.

Figure 5(a) shows the weight loss by nitridation of β-Ga_2O_3 at various P_{NH3} at 800 °C. These results indicate that the weight loss proceeds linearly to −8% ~ −10.8 %. The nitridation rate constant was calculated from the slope of the straight line approximation of the curves. A linear relationship exists between the rate constants and P_{NH3} (Fig. 5(b)). The nitridation of as-received and coarse β-Ga_2O_3 powders measured by isothermal TGA at 800 °C was compared (Fig. 6). At an early stage (0% to −3%), the nitridation rate for coarse β-Ga_2O_3 powder was slower than that of the as-received one; however, the two were almost the same at a middle stage (−3% to −8%). The surface area of the as-received β-Ga_2O_3 powder was about ten times larger than that of the coarse powder, hence the slower rates for the coarsened

sample at the early stage is because of its smaller surface area.

3.2 Microstructural observation

Figure 7 shows SEM photographs of coarse β-Ga_2O_3 particles nitrided at various weight losses. The un-nitrided coarse β-Ga_2O_3 particles have a smooth surface with stepped hexagonal plates (Figs. 7 (a) and (a')). At −0.3% weight loss, very small particles (~5 nm) are formed on the surface of the coarse β-Ga_2O_3 particles (Figs. 7 (b) and (b')); the number and size of these particles on the coarse β-Ga_2O_3 increases with nitridation (Figs. 7(c)–(f)). Since the samples of −1.8 to −8.1% weight loss exhibited the GaN peaks in XRD, the deposited particles must be GaN. At –5.8 and −8.1% weight loss, the triangle rectangular particles are piled up on sloughs of Ga_2O_3, forming hollow or tubular aggregates GaN (Figs. 7(e) and (f)).

3.4 Nitridation mechanism

We propose, based on the kinetic results and microstructural observations, a nitridation mechanism consisting of four steps as shown in Fig. 8, in the temperature range of 800–1000 °C. First, Ga_2O (g) is formed by the reaction between β-Ga_2O_3 (s) and H_2 and/or H-containing reactive species formed by the thermal decomposition of NH_3 (Fig. 8 (a)). NH_3 is mostly decomposed to H_2 and N_2 at ~1000 °C under equilibrium conditions; however, a

previous study found that the decomposition of NH_3 was about 10% or lower at around 1000 °C in an open flow system.[19] Other studies suggest that some reactive intermediate species, such as H, NH, or NH_2 radicals, are formed during the thermal decomposition of NH_3. [6, 8] From non-isothermal TG results (Fig. 2), decomposition of β-Ga_2O_3 to Ga_2O(g) by H_2 (eq. 2) in an H_2/Ar (40/60 kPa) atmosphere starts above 800 °C, showing that H_2 and/or the reactive intermediate species containing H formed by thermal decomposition of NH_3 can react with β-Ga_2O_3 (s) to form Ga_2O (g). In the second step (Fig. 8 (b)), Ga_2O (g) reacts with NH_3 resulting in the deposition of nano-sized GaN particles on surface of the β-Ga_2O_3 particles given as follows:

$$Ga_2O\ (g) + 2NH_3 \rightarrow 2GaN + H_2O + 2H_2 \quad (4)$$

The reaction (Eq. (4)) controls the nitridation of β-Ga_2O_3, as shown in Figs. 4 and 5, because the nitridation proceeds linearly with time and the nitridation rate depends linearly on P (NH_3). As nitridation progresses, the number and size of deposited GaN particles increases with the coagulated particles. At the third step (Fig. 8 (c)), such coagulated GaN particles are in triangular and rectangular shapes covering the starting β-Ga_2O_3 particles. H_2 and/or H-containing species are free to move into a Ga_2O_3 particle through GaN walls to form Ga_2O (g); however, the gas is confined inside GaN walls leading to an increase in the internal

pressure. As a result of Ga_2O (g) escaping, the GaN forms tubes or hollows (Fig. 8 (d)). Once an exit is created, the reaction (Eq. (4)) proceeds linearly in proportion to P (NH_3). In this reaction sequence, Ga_2O is supposed to be instable at room temperature or to be transported in short distance, because gas species containing Ga was not detected in exhaust gas of TG system.

4. Summary

The kinetics of nitridation of β-Ga_2O_3 to wurtzite-type GaN in an NH_3/Ar atmosphere was studied by TGA and microstructural observation. Non-isothermal TGA, nitridation of β-Ga_2O_3 started at ~650 °C; followed by the decomposition of GaN at ~1100 °C. The kinetic results by isothermal TGA showed that the nitridation of Ga_2O_3 follows linear kinetics; suggesting that the rate-limiting step is an interfacial reaction. From microstructural observation, it was observed that nano-sized GaN particles were deposited on the surface β-Ga_2O_3 in an early stage, which increased with time, and that the coagulated GaN particles cover the Ga_2O_3 particles. We speculate that the reaction of β-Ga_2O_3 with H_2 and/or H containing species gas from NH_3 produces Ga_2O (g); the latter reacts with NH_3 to form GaN.

Acknowledgment

This work was supported in part by the Global COE Program (Project No. B01: Catalysis as the Basis for Innovation in Materials Science) from the Ministry of Education、 Culture、 Sports、 Science and Technology、 Japan)

References

[1] R. P. Vaudo, D. Goepfert, T. D. Moustakas, D. M. Beyea, T. J. Frey and K. Meehan,. *J. Appl. Phys.,* **79**(1996) 2779-2783.

[2] G. Jacob and D. Bois, *Appl. Phys. Lett.*, **30** (1977) 412-414.

[3] S. J. Pearton and F. Ren, *Advanced Materials*, **12** (2000)1571.

[4] A. Addamiano, *J. Electrochem. Soc.*, **108** (1961) 1072-1072.

[5] B. B. Binkowski and M. R. Lorent, *J. Electrochem. Soc.*, **109** (1962) 24-26.

[6] C. M. Balkas and R. F. Davis, *J. Am. Ceram. Soc.*, **79**[9] (1996) 2309-2312.

[7] H. D. Xiao, H. L. Ma, C. S. Xue, J. Ma, F. J. Zong, X. J. Zhang, F. Ji and W. R. Hu, *Mater. Chem. Phys.*, **88** (2004) 180-184.

[8] L. Q. Luo, K. Yu, Z. Q. Zhu, Y. S. Zhang, H. L. Ma, C. S. Xue, Y. G. Yang and S. Q. Chen, *Mater. Lett*, **58** (2004)2893-2896.

[9] S. Ohira, M. Yoshioka, T. Sugawara, K. Nakajima and T. Shishido, *Thin Solid Films*, **496** (2006) 53-57.

[10] J. Dinesh, M. Eswaramoorthy and C. N. R. Rao, *J. Phys. Chem. C*, **111** (2007) 510-513.

[11] H. J. Lee, T. I. Shin and D. H. Yoon, *Surf. Coat. Tech.*, **202** (2008) 5497-5500.

[12] S. Shimada and R. Taniguchi, *J. Cryst. Growth*, **263** (2004)1-3.

[13] S. Shimada, Y. Miura, A. Miura and T. Sekiguchi, T. *Cryst. Growth. Des.*, **7** (2007) 1251-1255.

[14] A. Miura, S. Shimada, M. Yokoyama, H. Tachikawa and T. Kitamura, *Chem. Phys. Lett.*, **451** (2008) 222-225.

[15] A. Miura, S. Shimada, T. Sekiguchi, M. Yokoyama and B. Mizobuchi, B. *J. Cryst. Growth*, **310** (2008) 530-535.

[16] W. S. Jung, *Mater Lett*, **60** (2006) 2954-2957.

[17] W. S. Jung, O. H. Han and S. A. Chae, *Mater. Chem. Phys.*, **100** (2006)199-202.

[18] D. P. Butt, Y. Park and T. N. Taylor, *J. Nucl. Mater.*, **264** (1999) 71-77.

[19] H. Lee and J. S. Harris, *J. Cryst. Growth*, **169** (1996) 689-696.

Figures captions

Fig. 1. SEM photographs of (a) as-received and (b) coarse β-Ga_2O_3 powder. The coarsened sample was fabricated by heating as-received sample at 1400 °C for 1 h. Insets are magnified images.

Fig. 2. Non-isothermal TGA curves of as-received β-Ga_2O_3 powder against temperature in NH_3/Ar, H_2/Ar, and Ar atmospheres.

Fig. 3. XRD patterns of (a) as-received β-Ga_2O_3 and the sample obtained by non-isothermal nitridation up to (b) 870 °C and (c) 1200 °C.

Fig. 4. TGA curves obtained by isothermal experiments of β-Ga_2O_3 in Ar/NH_3 (50/50) atmosphere at the temperatures of (a) 800 °C, (b) 900 °C, and (c) 1000 °C. Dashed lines superimposed on the TGA curves show the slope of each curve. A horizontal dotted line shows the calculated weight loss based on the complete nitridation of β-Ga_2O_3.

Fig. 5. (a) Isothermal TGA curves of the fine sample at 800 °C at various $P(NH_3)$. Dashed

lines superimposed on the TGA curves show the slope of the each curve, and the horizontal dotted line, theoretical weight loss. (b) Plots of rate constants obtained from TGA results as a function of P_{NH3}.

Fig. 6. Comparison of isothermal TGA curves between (a) as-received and (b) coarse β-Ga_2O_3 powder at 800 °C in Ar/NH_3 atmosphere. Dashed lines superimposed on the TGA curves show the slope of each curve. The horizontal dotted line shows the calculated weight loss based on the complete nitridation of Ga_2O_3.

Fig. 7. SEM photographs of partially nitrided coarse β-Ga_2O_3 powder at 800 °C. Weight changes of the partially nitrided samples are (a) 0%, (b) −0.3%, (c) −1.8%, (d) −3.5%, (e) −5.8%, and (f) −8.1%; (a'), (b'), and (f') are magnified images of (a), (b), and (f), respectively.

Fig. 8. A model for formation of GaN from β-Ga_2O_3 in an NH_3 atmosphere: (a) formation of Ga_2O (g), (b) formation of GaN depositions on β-Ga_2O_3; (c) growth of GaN; and (d) formation of hollow or tubular GaN aggregates.

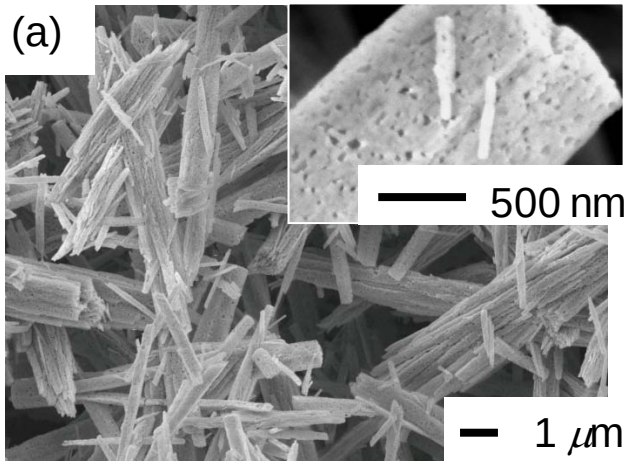

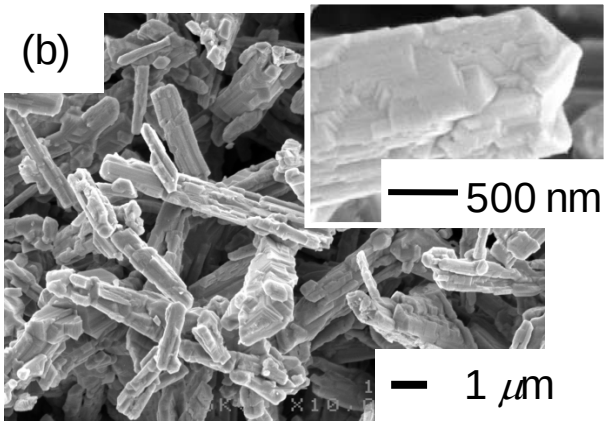

Fig. 1

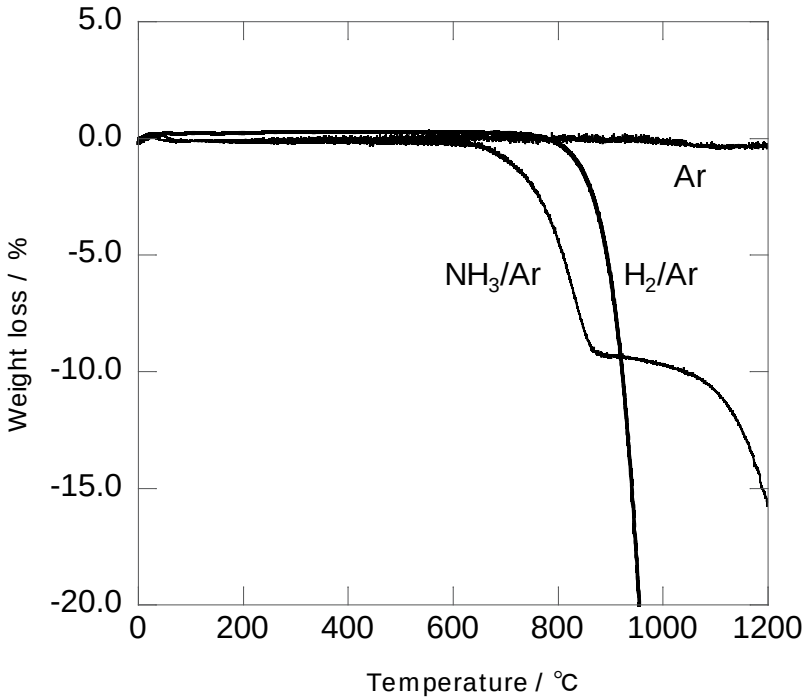
5.0
0.0
-5.0
-10.0
-15.0
-20.0
0
200
400
600
800
1000
1200
Weight loss / %
Temperature / ℃
Ar
NH3/Ar
H2/Ar

Fig.2

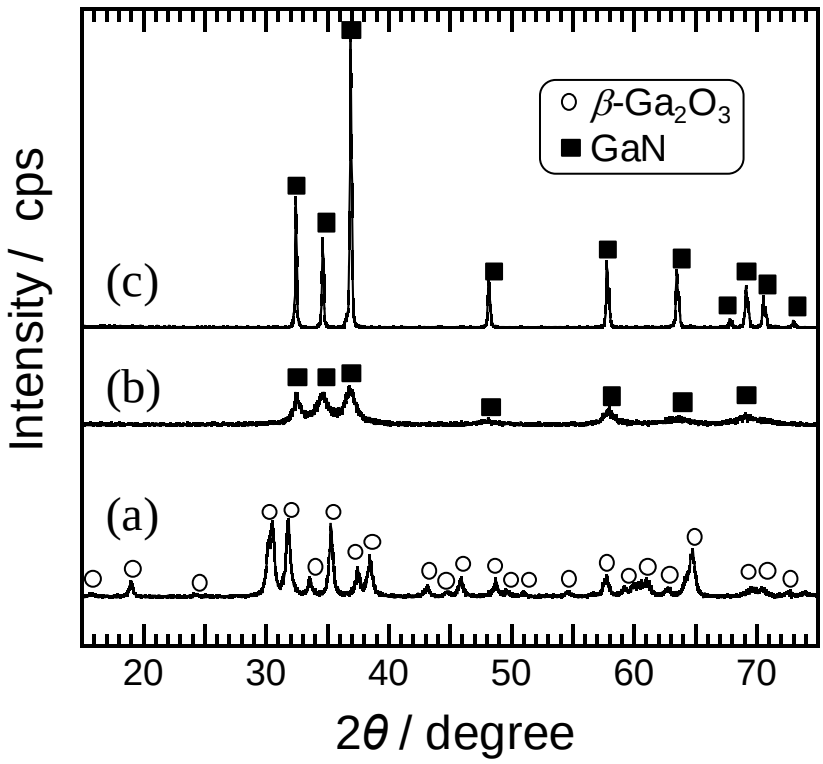

Fig.3

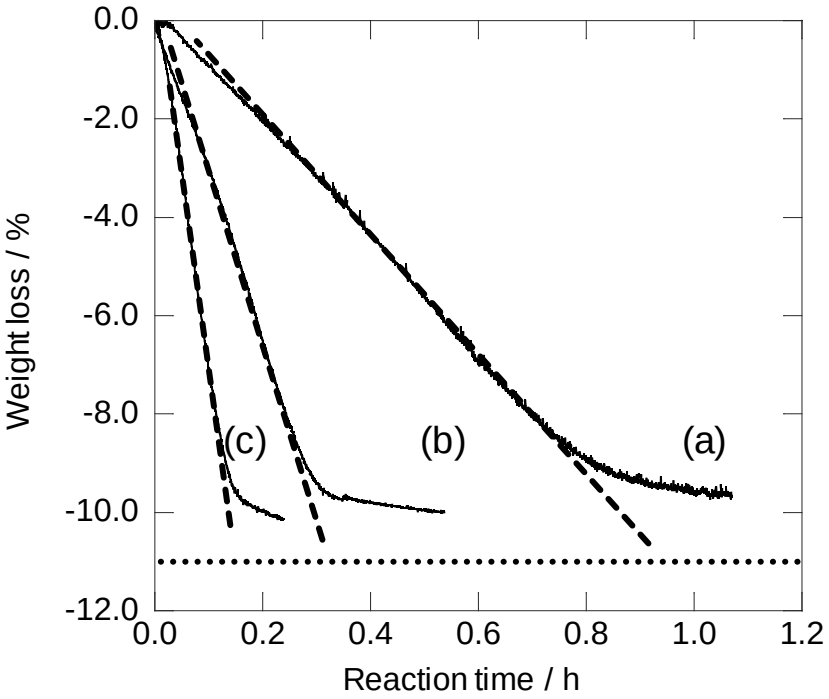
0.0
-2.0
-4.0
-6.0
-8.0
-10.0
-12.0
Weight loss / %
0.0
0.2
0.4
0.6
0.8
1.0
1.2
Reaction time / h
(a)
(b)
(c)

Fig.4

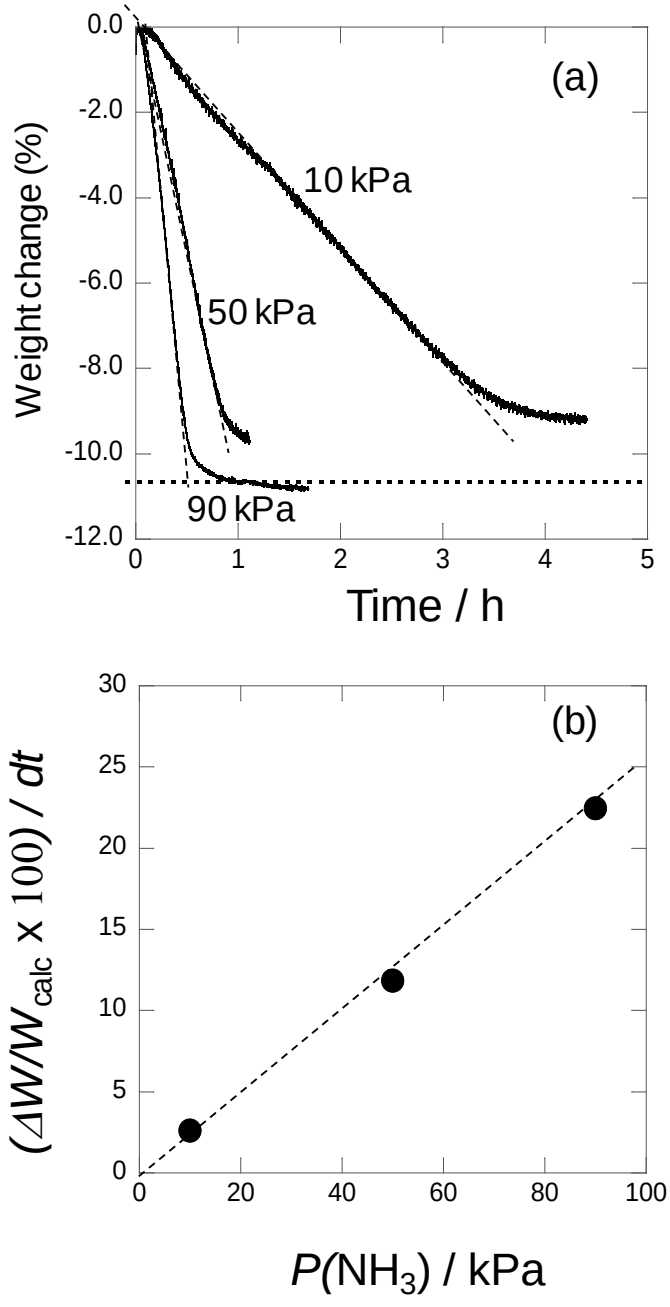
(a)
Weight change (%)
0.0
-2.0
-4.0
-6.0
-8.0
-10.0
-12.0
10 kPa
50 kPa
90 kPa
0
1
2
3
4
5
Time / h
(b)
(ΔW/W_calc x 100) / dt
30
25
20
15
10
5
0
0
20
40
60
80
100
P(NH3) / kPa

Fig.5

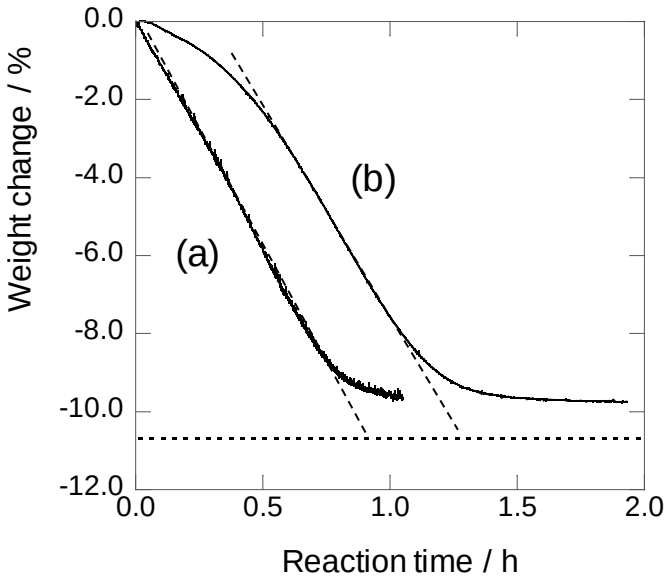
0.0
-2.0
-4.0
-6.0
-8.0
-10.0
-12.0
0.0
0.5
1.0
1.5
2.0
Weight change / %
Reaction time / h
(a)
(b)

Fig.6

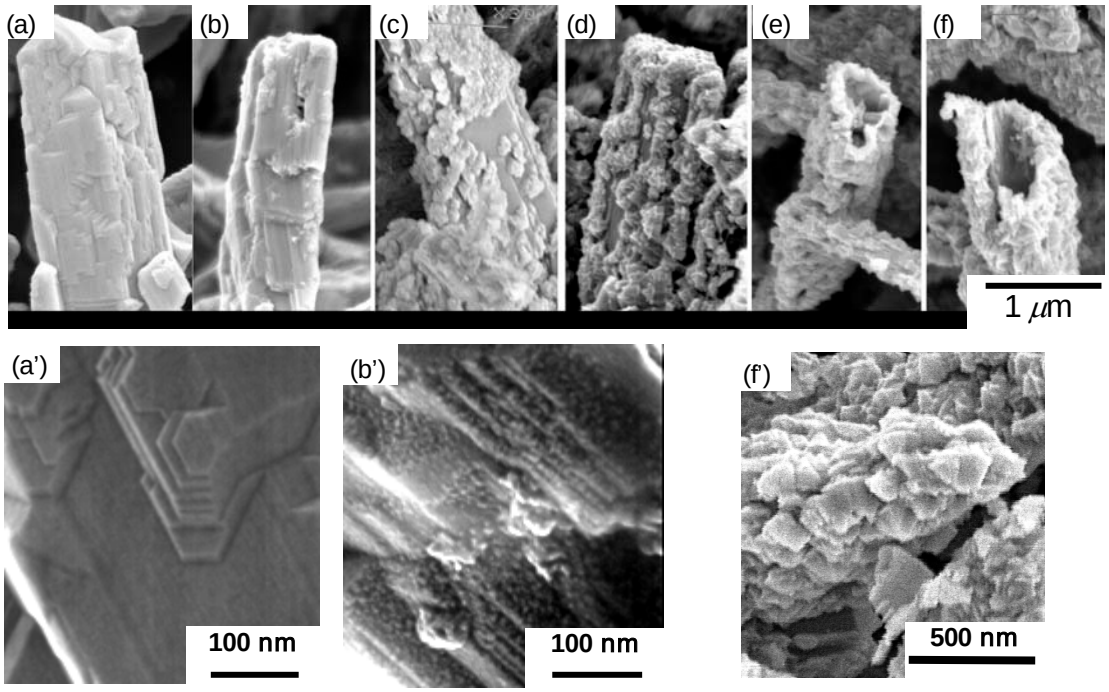

Fig.7

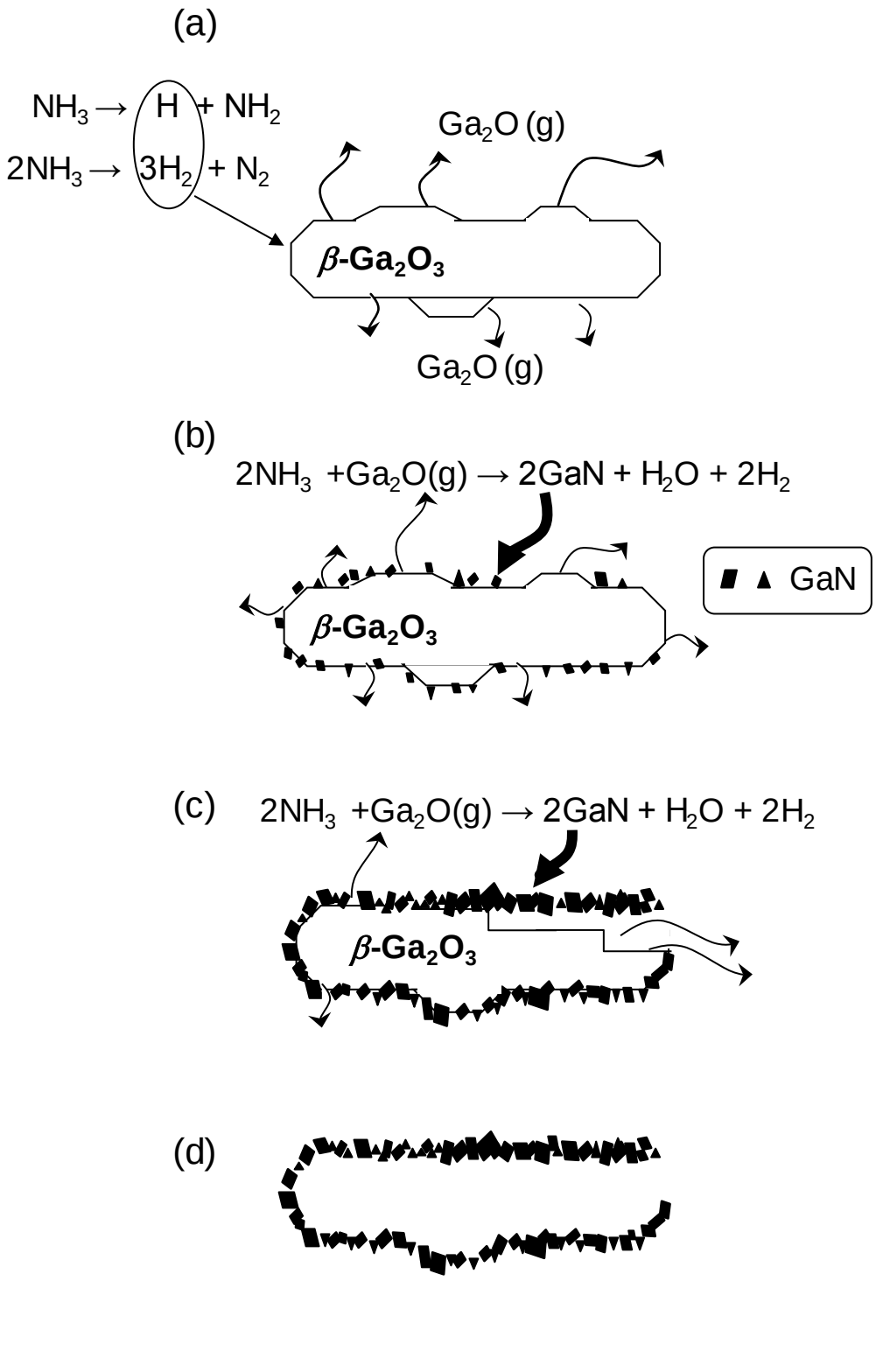
(a)
NH3 → H + NH2
2NH3 → 3H2 + N2
Ga2O (g)
β-Ga2O3
Ga2O (g)
(b)
2NH3 +Ga2O(g) → 2GaN + H2O + 2H2
GaN
β-Ga2O3
(c)
2NH3 +Ga2O(g) → 2GaN + H2O + 2H2
β-Ga2O3
(d)

Fig.8